Journal of Solid State Chemistry 183 (2010) 2714–2719

Contents lists available at ScienceDirect

Journal of Solid State Chemistry

journal homepage: www.elsevier.com/locate/jssc

Fluorescence line narrowing spectroscopy of Eu^{3+} in zinc–thallium–tellurite glass

V.P. Tuyen [a,1], T. Hayakawa [a,b,c,*], M. Nogami [a], J.R-. Duclère [b], P. Thomas [b]

[a] Fields of Advanced Energy Conversion, Department of Frontier Materials, Nagoya Institute of Technology, Gokiso-cho, Showa-ku, Nagoya 466-855, Japan
[b] Science des Procedes Ceramiques et de Traitements de Surface (SPCTS), UMR 6638 CNRS, Faculte des Sciences, Universite de Limoges, 123 avenue Albert Thomas, 87060 Limoges Cedex, France
[c] Toyota Physical and Chemical Research Institute, 41-1 Yokomichi, Nagakute, Aichi 480-1192, Japan

ARTICLE INFO

Article history:
Received 2 May 2010
Received in revised form
10 August 2010
Accepted 18 August 2010
Available online 22 August 2010

Keywords:
Tellurite glass
Europium
Crystal field parameters
Fluorescence line narrowing
Asymmetry

ABSTRACT

The environment of Eu^{3+} in zinc–thallium–tellurite glass of the molar composition $60TeO_2$–$30TlO_{0.5}$–$9.9ZnO$–$0.1Eu_2O_3$ was investigated by laser-induced fluorescence line narrowing (FLN) techniques using Eu^{3+} as a local site probe. From the site selective luminescence spectra of Eu^{3+} at 7 K, the energies of the Stark components of the $^7F_1$ and $^7F_2$ states were recorded and then the crystal field parameters B_{nm} were calculated assuming a C_{2v} site symmetry. The ratios B_{22}/B_{20} and B_{44}/B_{40} for each excitation energy within $^7F_0$–$^5D_0$ transition were obtained and compared with the values calculated for Eu^{3+} in other types of glasses.

1. Introduction

Recently, a novel glass system of zinc–thallium–tellurite has been developed as a photonic material in our collaborative research project, and its second- and third-order nonlinearities were reported [1–3]. Zinc–thallium–tellurite glasses are supposed to be more attractive, especially when doped with luminescent lanthanide ions for photonic devices or communication systems. Since they are characterized by good chemical stability, homogeneous distribution of lanthanide ions, lower maximum vibration frequencies (650–750 cm^{-1}) reducing the multiphonon relaxation, and nonlinear optical responses, [4–7] the new photonic glasses are potential to improve optical absorption/emission cross-sections of these optically active ions.

The optical spectroscopy of zinc–thallium–tellurite glasses activated with Eu^{3+} ions is quite new (not reported so far) so that it is valuable to study the local structure around Eu^{3+} ions in zinc–thallium–tellurite glass by crystal-field analyses of fluorescence-line narrowing (FLN) spectra [8]. The narrow spectral bandwidth of a dye laser has been used to excite only a small subset of Eu^{3+} ions out of the full ensemble of sites occupied in the glass. By tuning the laser frequency over the inhomogeneous bandwidth of $^7F_0$–$^5D_0$ transition different Eu^{3+} sites were sampled. Hence, this technique has become the most powerful experimental tool for the study of local structural inhomogeneties of lanthanide ions in glasses.

Excitation of the nondegenerate $^7F_0 \rightarrow {}^5D_0$ transition leads to $^5D_0$ fluorescence terminating on levels belonging to the ^7F_J ($J=0$, 1, …, 6) multiplets. The multiplets are $2J+1$ degenerate and thus can be split into a maximum $2J+1$ Stark components depending on the symmetry of the crystal field. Such transitions are parity forbidden in free ion for electric dipole processes. However, in a glass, these transitions are allowed as a consequence of coupling introduced by odd-parity terms in the crystal-field expansion [9,10]. The structure observed in the fluorescence spectrum (number of peaks) is then determined only by the splitting of the terminal levels caused by the local crystal field, because no Stark splitting of the emitting $^5D_0$ state can occur under any symmetry. Furthermore, the splitting of the terminal levels is very sensitive to local variations in the crystal field.

In this study, the environment of Eu^{3+} in $60TeO_2$–$30TlO_{0.5}$–$9.9ZnO$–$0.1Eu_2O_3$ glass was investigated by FLN techniques. The molar composition was determined on the basis of our previous reports [1–3]. From the energies of the Stark components of the $^7F_1$ and $^7F_2$ states recorded, the crystal field parameters B_{nm} were calculated assuming a C_{2v} site symmetry. Moreover, the ratios

* Corresponding author at: Fields of Advanced Energy Conversion, Department of Frontier Materials, Nagoya Institute of Technology, Gokiso-cho, Showa-ku, Nagoya 466-855, Japan. Fax: +81 52 735 5110.
E-mail address: hayatomo@nitech.ac.jp (T. Hayakawa).
[1] Present address: Institute of Materials Science-Vietnam Academy of Science and Technology, 18 Hoang Quoc Viet Road, Cau Giay, Hanoi, Vietnam.

0022-4596/$ - see front matter © 2010 Elsevier Inc. All rights reserved.
doi:10.1016/j.jssc.2010.08.025

B_{22}/B_{20} and B_{44}/B_{40} for each excitation energy within $^7F_0$–$^5D_0$ transition were obtained and compared with the values calculated for Eu^{3+} in other types of glasses.

2. Experimental

Zinc–thallium–tellurite glass of molar composition $60TeO_2$–$30TlO_{0.5}$–9.9ZnO–$0.1Eu_2O_3$ was prepared by melting a mixture of the reagents TeO_2, Tl_2CO_3, ZnO, and Eu_2O_3 powders in a platinum crucible for 20 min at 800 °C in an ambient atmosphere. Tl_2CO_3, ZnO, and Eu_2O_3 were commercial products. TeO_2 fine powder was obtained by a thermal decomposition of orthotelluric acid (H_6TeO_6, Aldrich, 99.9%) at 560 °C for 24 h [1]. The melts were quenched down to ~100 °C in a brass ring mold on a brass base to obtain cylindrical samples of ϕ1.0 cm in diameter and 1.5 mm in thickness. The samples were then polished to obtain planar disks suitable and cleaned with acetone for optical measurements.

The broad-band emission spectrum was recorded at room temperature in the range 550–750 nm by exciting the sample at an excitation of 467 nm using a 500 W xenon lamp passed through a monochromator (Jobin Yvon, H20-UV). The fluorescence line narrowing measurements were conducted by a tunable dye laser (Coherent, Model 599) operating with rhodamine 6G pumped by an diode-pumped solid state (DPSS) laser (Coherent, Verdi-V5) to provide the tunable radiation selectively exciting the $^7F_0 \rightarrow {}^5D_0$ transition of Eu^{3+}. The laser had a linewidth (full width at half maximum) of 1.0 cm^{-1} over the tuning range 17,198–17,276 cm^{-1} used in this work. The luminescence signal was monitored with a monochromator (Jobin Yvon, HR-320) equipped with an optical double chopper, a Hamamatsu R955 photomultiplier and a lock-in amplifier (EG&G, 5209) and recorded under a computer control software [11]. Low temperature data were acquired at 7 K using a helium closed-cycle cryostat. Overlapping bands were separated by deconvoluting the measured spectra with Gaussian bands in a least-squares minimization routine. The relative measuring error was estimated to be about 1%. The crystal field parameters were obtained from the experimental energy levels of the Stark components.

3. Results and discussion

Fig. 1 shows a broad-band emission spectrum of the Eu^{3+} ions in $60TeO_2$–$30TlO_{0.5}$–9.9ZnO–$0.1Eu_2O_3$ glass excited at 467 nm at room temperature. This excitation energy is expected so that the full ensemble of Eu^{3+} ions can be excited by the light via $^5D_2$ level, which has energy greater than that necessary to excite the $^5D_0$–^7F_J emission. This is obtained firstly by nonradiative relaxation from energy level of $^5D_2$ to $^5D_0$ and then by emission to the ^7F_J multiplets. The emission spectrum consists of five groups of emission bands at about 579, 592, 613, 653, and 702 nm. The five groups are due to the transitions from $^5D_0$ to ^7F_J (J=0, 1, 2, 3, 4).

$^5D_0 \rightarrow {}^7F_1$ is a magnetic dipole transition and its intensity hardly varies with the bonding environment of the Eu^{3+} ions while $^5D_0 \rightarrow {}^7F_2$ is an electric allowed transition, which is hypersensitive to the coordination environment of Eu^{3+} ions. The intensity ratio (R) of $^5D_0 \rightarrow {}^7F_2$ to $^5D_0 \rightarrow {}^7F_1$ is thus used to estimate the deviation from the site symmetries of Eu^{3+} ions. Besides that, the variation of R and a Judd–Ofelt's phenomelogical parameter Ω_2 [9,10] are of the same trend because the probability of $^5D_0 \rightarrow {}^7F_2$ transition is solely determined by Ω_2. It is reported by Arafin [12] and Kumar [13] that Ω_2 parameter is very high in tellurite glass ($\Omega_2 \sim 11 \times 10^{-20}$ to 12×10^{-20} cm^2) in comparison with other host materials (silicate: $\Omega_2 \sim 6 \times 10^{-20}$ to 8×10^{-20} cm^2, fluorite: $\Omega_2 \sim 0.05 \times 10^{-20}$ to 1.2×10^{-20} cm^2), regarding to noncentrosymmetric structures of tellurite units [14]. Therefore, the increase in R (that means increasing Ω_2) is due to a degree of asymmetry of ligand or oxygen coordination in oxide glasses.

The ratio R is also used to estimate the luminescence efficiency of the luminescence band $^5D_0 \rightarrow {}^7F_2$ of the material, because the intensity of the luminescence band $^5D_0 \rightarrow {}^7F_1$ is independent of luminescence materials, which is usually used as the internal standard to estimate the luminescence efficiency of the material as the phosphor for the red luminescence (613 nm). The value of R in zinc–thallium–tellurite glass is found to be 3.4, which lies high value within the range 2–4 found in oxide glasses as evidence to indicate that Eu^{3+} ions in zinc–thallium–tellurite glass occupy relatively low-symmetry sites [15]. This value of R is equivalent with that of lithium borate glass doped with a much larger amount of Eu_2O_3 (2%) [16]. This therefore indicates that Eu^{3+} doped zinc–thallium–tellurite glasses are promising as a red light source.

Low-temperature FLN spectra obtained at 7 K for the glass $60TeO_2$–$30TlO_{0.5}$–9.9ZnO–$0.1Eu_2O_3$ are shown in Fig. 2. The exact positions of the different excitation wavenumber are represented in the figure. All of them are inside the $^7F_0$–$^5D_0$ absorption band, which closely corresponds to the respective emission band $^5D_0$–$^7F_0$ due to the small Stocks's shift usually observed in f–f

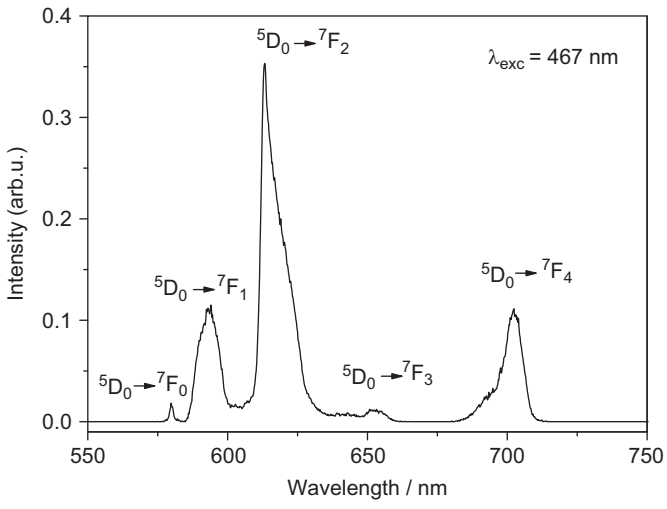

Fig. 1. Broad-band fluorescence spectrum of $60TeO_2$–$30TO_{0.5}$–9.9ZnO–$0.1Eu_2O_3$ glass at room temperature.

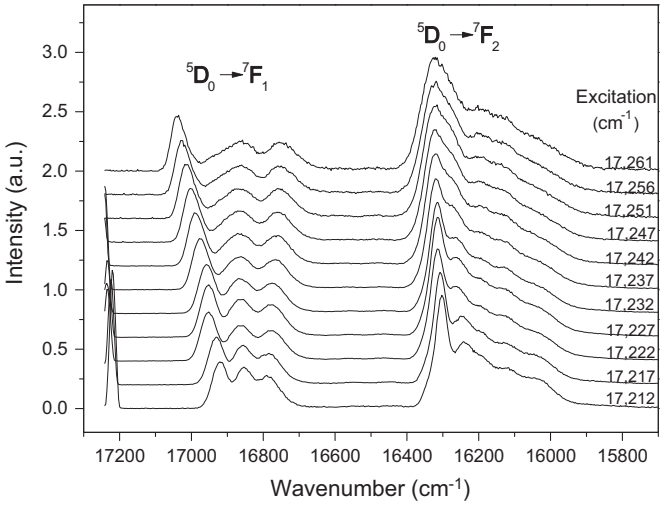

Fig. 2. Low temperature FLN spectra of $60TeO_2$–$30TlO_{0.5}$–9.9ZnO–$0.1Eu_2O_3$ glass at 7 K.

transitions of lanthanide ions. The full widths at half maximum for the $^5D_0$–$^7F_0$ were found to be about 100 cm^{-1} for the oxide glass [17]. With increasing excitation energy still further, a weak but invariant typical luminescence corresponding to $^5D_0$–$^7F_1$ and $^5D_0$–$^7F_2$ transitions are still visible. This persists at excitation energy well away from the $^5D_0$ absorption band. These spectra are caused by excitation into the broad phonon sideband (PSB) situated to the high energy side of the pure electronic (PE) $^5D_0$ level [18].

However, in our experiment, the excitation was limited to a narrow wavenumber range around the band center (17,198–17,276 cm^{-1}) in order to avoid nonselective excitation caused by phonon side band absorption [19]. It is evident that the splittings of the Stark components are very visible, in particular, the splitting of the $^7F_1$ state tends to become larger when the excitation energy increases. The higher and lower energy components of the $^5D_0$–$^7F_1$ emission shows a strong excitation-dependent shift in energy and a remarkable narrowing, whereas the other component remains relatively constant, in agreement with Brecher and Riseberg [20]. In our experiment, the high resolution of the Stark components and the clear presence of three peaks in the $^5D_0$–$^7F_1$ emission even for higher excitation energies, are due to the absence of the PSB absorption [19].

In our experiment the five Stark splitting components of the $^7F_2$ level are also observed, in particular, for the lower energy excitation. However, the five Stark components of the $^5D_0$–$^7F_2$ transition are not clearly observable in the materials, which exhibit the broad width of the individual Stark components [17].

The energies of the $^7F_1$ and $^7F_2$ Stark levels were obtained from FLN spectra using a Gaussian deconvolution routine, as shown in Fig. 3. Fig. 4 compiles the results as a function of the excitation energy. It is evident that, in this case, the variations of the Stark levels, especially the Stark levels of $^7F_2$, depend weakly on the excitation energy. Note this difference compared to that found for some other glasses, especially fluorite glasses. The crystal field parameter values are affected by the distances, bonding angles, and the nature of ligands (including the electronegativity, the covalence degree, etc.) that characterize the crystallographic site of the rare-earth ion. The electronegativity (in Pauling scale) of the oxygen and fluorine are 3.44 and 3.98. Therefore, the degree of covalency in the Eu–O bond should be more than that in Eu–F bond. These differences lead to the differences in the coordination configuration of the Eu–O bond and Eu–F systems. According to

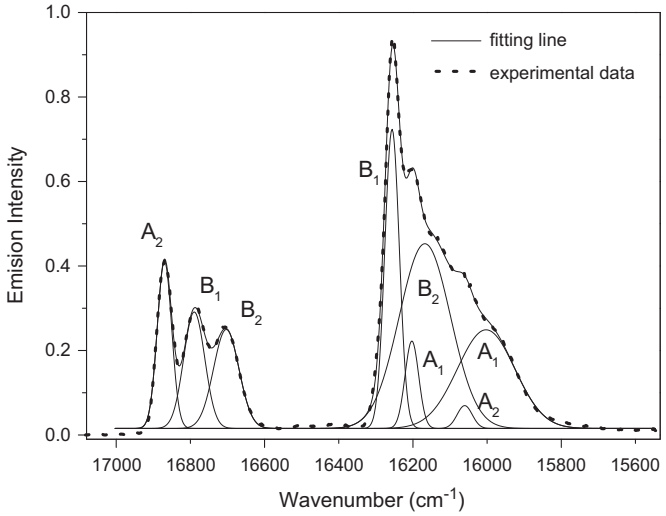

Fig. 3. Spectra using a Gaussian deconvolution routine. The labels, A_1, A_2, B_1, B_2, are representive indexes of C_{2v} point group.

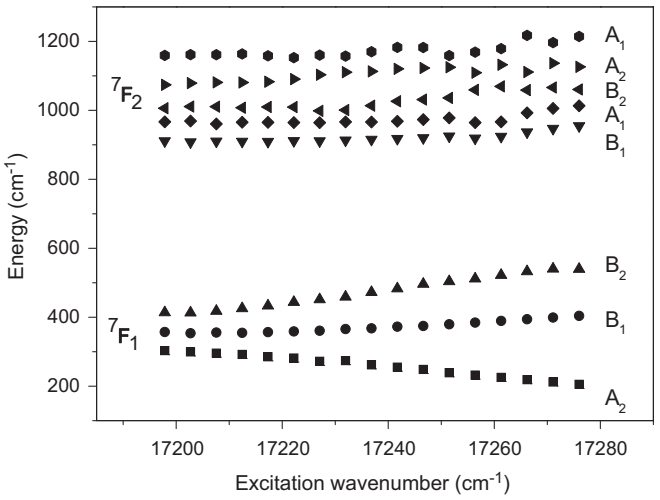

Fig. 4. Energies of the Stark levels of the $^7F_1$ and $^7F_2$ multiplets for the glass with the composition $30TlO_{0.5}$–$60TeO_2$–9.9ZnO–$0.1Eu_2O_3$. The labels, A_1, A_2, B_1, B_2, are representive indexes of C_{2v} point group.

the study of Brecher and Riseberg [20], the structural model derived for oxide glasses was found to be inadequate to explain the observed behaviors of the fluoride glass, but an alternate model was proposed, this model involved a ninefold coordination of Eu by two set of nonequidistant fluoride ions and a systematic axial distortion for this arrangement. The differences can be attributed to the chemical difference between oxygen and fluorine themselves. The degree of covalency in the metal–oxygen bond should be considerably more than in the metal–fluorine bond. Indeed, the fluoberyllate network studied by Brecher and Riseberg [21] is considered to be almost totally ionic in nature. In the tellurite glass, the excitation-dependent pattern of the Stark splittings has revealed the demonstrated similarities in the spectroscopic behavior of Eu^{3+} in a wide variety of oxidic glasses, which is not directly carried over into fluoridic analogs.

Following the arguments of Brecher and Riseberg [20], the crystal-field calculations are based on the assumption of C_{2v} point symmetry, which is customarily employed for the crystal field analysis of site selective spectra of Eu^{3+} in glasses, where the labels, A_1, A_2, B_1, B_2, used in Figs. 3 and 4, are representive indexes of C_{2v} point group. This symmetry is the highest noncentrosymmetric for which full Stark splitting of the J manifolds occurs (highest symmetry with no degenerate representations) and the lowest symmetry for which symmetry distinctions of most of the components are maintained. Lempicki et al. [22] gave the Hamiltonian (H_c) for performing the crystal-field form in terms of the operator equivalents O_{nm}

$$H_c = \sum_n \sum_m \theta_J^{(n)} [B_{nm}^c O_{nm}^c + B_{nm}^s O_{nm}^s] \tag{1}$$

$$B_{nm}^{c,s} = A_{nm}^{c,s} \langle r^n \rangle = -|e| K_n \langle r^n \rangle \gamma_{nm}^{c,s} \tag{2}$$

where the quantities B_{nm} are the crystal field parameters and the factors $\theta_J^{(n)}$ are the operator equivalent constants α_J, β_J and γ_J for $n=2$, 4, and 6, respectively; K_n is a normalizing factor; and $\gamma_{nm}^{c,s}$ are the lattice sums. The various entries in the secular determinant are

$$\langle JM|H_c|JM'\rangle = H_{MM'} \tag{3}$$

Using the equations for C_{2v} symmetry [22], a set of crystal-field parameters, B_{nm}, giving a best fit to all eight components, was

derived for each spectrum. The best fit was determined by using a Gauss–Newton algorithm to minimize the sum of squared residuals between the observed and calculated peak positions. The fits for spectra obtained from the glass using the symmetry assignments of Brecher and Riseberg were very good with a root mean squared (rms) errors between the fitted and observed peak positions $< 10\%$ (Table 1).

The crystal field parameters B_{20}, B_{22}, B_{40}, B_{42}, and B_{44} are plotted in Fig. 5 for the glass $60TeO_2$–$30TlO_{0.5}$–9.9ZnO–$0.1Eu_2O_3$ as a function of the excitation wavenumber. The dependence of the B_{nm} values on the excitation wavenumber is qualitatively similar to those observed in germanate glasses [23] and in other glasses such as silicate [20,24], phosphate [17], and borate [25] glasses.

To receive the information about the symmetry of crystal field surrounding the emitting ion, it is necessary to extract the angular components from the crystal parameters B_{nm} in Fig. 4. For that, the major crystal field ratios B_{22}/B_{20} and B_{44}/B_{40}, which are sensitive to the angular positions of the oxygen ligands [20] were calculated for each FLN spectrum from the crystal field parameters and compared with the ones calculated by Brecher and Riseberg on the basis of their geometric model (BR model) proposed for Eu^{3+} sites in oxide glasses. This model involves the progressive approach of a ninth ligand to an originally eightfold coordinated site having symmetry C_{2v}.

Fig. 6 shows the comparison between the experimental CF-ratios B_{22}/B_{20} and B_{44}/B_{40} and the values calculated according to the BR structure model [20]. A plot of ratio B_{44}/B_{40} as a function of $-B_{22}/B_{20}$ shows that the experimental points are close to the behavior predicted by the BR model. The experimental points determined in this research agree well with the theoretical BR prediction on the shape of the curve. This is, firstly, to indicate that the BR model could describe acceptably the local structure around Eu^{3+} in the zinc thallium tellurite glass under investigation.

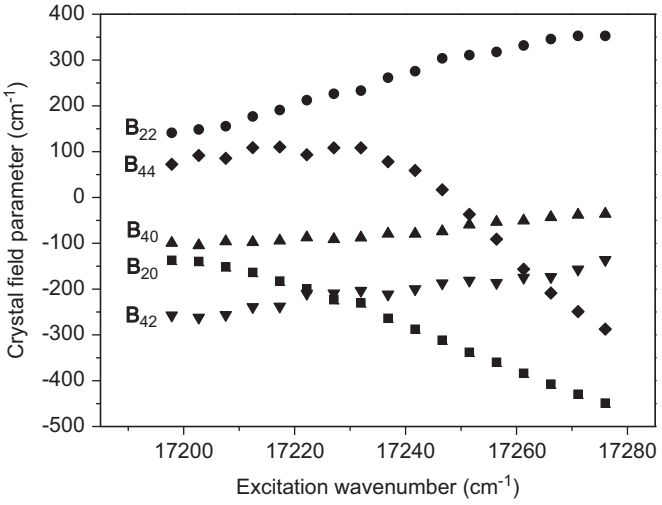

Fig. 5. Crystal field parameters for $60TeO_2$–$30TlO_{0.5}$–9.9ZnO–$0.1Eu_2O_3$ glass as a function of the excitation wavenumber.

Table 1
Energy levels of Eu^{3+} in zinc–thallium–tellurite glass ($60TeO_2-30TlO_{0.5}$–$9.9ZnO-0.1Eu_2O_3$) as functions of the excitation energy of $^7F_0$–$^5D_0$.

Excitation energy (cm^{-1})		$^7F_1$			$^7F_2$					
		A_2	B_1	B_2	B_1	A_1	B_2	A_2	A_1	rms/%
17,276	obs	205.3	404.1	545.2	954.8	1013.2	1063.3	1136.5	1204.0	0.8
	cal	205.3	404.1	545.2	954.8	1004.0	1063.3	1136.5	1213.2	
17,271	obs	212.1	399.1	540.3	947.2	1005.6	1061.0	1131.6	1196.5	0.2
	cal	212.0	399.2	540.3	947.3	1003.9	1061.0	1131.6	1198.2	
17,266	obs	218.8	394.2	532.6	937.0	992.8	1053.5	1124.1	1191.6	1.1
	cal	218.7	394.3	532.6	937.0	1004.1	1053.5	1124.1	1180.3	
17,261	obs	225.5	389.3	522.1	926.8	982.6	1040.7	1116.6	1181.5	2.1
	cal	225.5	389.3	522.1	926.7	1005.0	1040.7	1116.7	1159.1	
17,256	obs	232.2	384.4	511.6	924.5	977.7	1038.4	1116.9	1174.0	3.0
	cal	232.2	384.5	511.6	924.5	1009.2	1038.4	1116.9	1142.5	
17,251	obs	238.9	379.6	503.9	925.0	978.1	1036.2	1119.9	1171.7	3.8
	cal	238.9	379.6	503.9	925.0	1017.8	1036.2	1119.9	1132.0	
17,247	obs	248.5	374.7	496.2	920.1	973.2	1031.3	1122.8	1182.3	5.7
	cal	248.5	374.7	496.2	920.1	1034.0	1031.3	1122.8	1121.6	
17,242	obs	255.1	372.6	482.9	917.9	968.3	1026.4	1120.5	1180.0	6.9
	cal	255.1	372.6	482.9	917.9	1040.9	1026.4	1120.5	1107.5	
17,237	obs	261.8	367.7	472.4	915.6	966.1	1024.1	1113.0	1170.0	7.2
	cal	261.8	367.7	472.4	915.6	1041.5	1024.1	1113.0	1094.6	
17,232	obs	274.2	365.7	459.1	913.4	966.5	1014.0	1105.5	1162.5	8.0
	cal	274.1	365.7	459.1	913.4	1049.7	1014.0	1105.5	1079.3	
17,227	obs	272.2	360.8	451.4	911.2	964.3	1011.7	1103.2	1165.4	8.5
	cal	272.1	360.8	451.4	911.2	1053.0	1011.7	1103.2	1076.7	
17,222	obs	281.7	358.8	443.7	911.6	964.7	1009.5	1090.6	1152.8	8.3
	cal	281.6	358.8	443.7	911.7	1050.2	1009.5	1090.5	1067.2	
17,217	obs	285.4	356.8	433.2	909.4	965.1	1009.9	1090.9	1158.2	9.0
	cal	285.4	356.8	433.2	909.4	1058.3	1009.9	1090.9	1065.0	
17,212	obs	292.0	354.7	425.5	909.9	965.5	1007.6	1086.0	1158.5	8.8
	cal	291.9	354.7	425.5	909.9	1055.9	1007.6	1086.0	1068.1	
17,208	obs	295.7	355.5	417.8	910.3	960.6	1008.0	1078.5	1161.4	8.7
	cal	295.7	355.5	417.8	910.3	1050.8	1008.0	1078.6	1071.2	
17,203	obs	299.4	353.5	412.9	908.1	968.9	1005.8	1078.9	1161.6	7.9
	cal	299.4	353.5	412.9	908.1	1050.7	1005.8	1078.9	1079.9	
17,198	obs	303.1	357.2	413.7	911.2	966.7	1006.1	1074.0	1159.4	8.0
	cal	303.1	357.2	413.7	911.2	1049.6	1006.1	1074.0	1076.4	

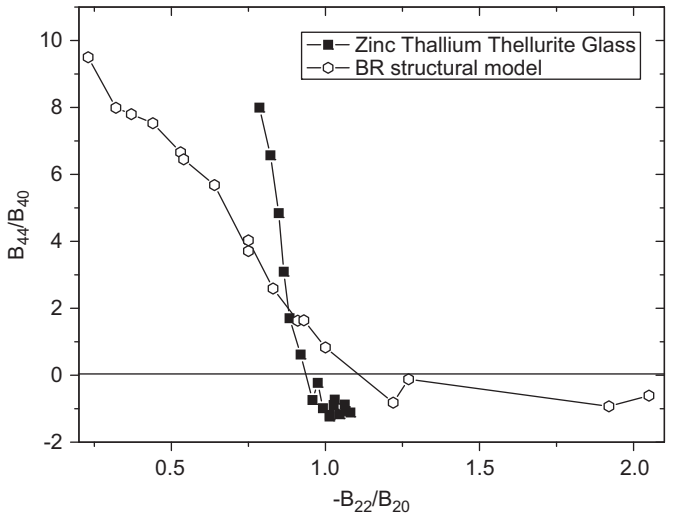

Fig. 6. Crystal field (CF) ratios B_{22}/B_{20} and B_{44}/B_{40} of Eu^{3+} doped zinc–thallium–tellurite glass calculated using the structural model proposed by Brecher and Riseberg (BR).

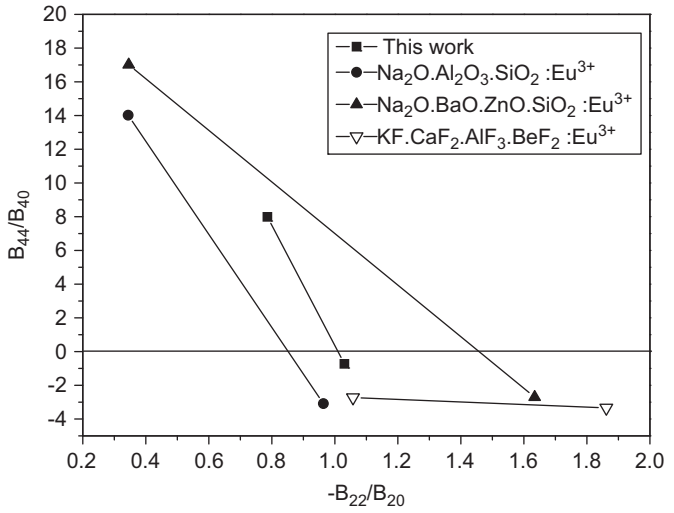

Fig. 7. Crystal field ratios $-B_{22}/B_{20}$ and B_{44}/B_{40} of some glasses doped with Eu^{3+} ions.

In order to estimate the role of the anions in the features of FLN spectra of the different glasses, a plot of ratios, B_{44}/B_{40} as a function of $-B_{22}/B_{20}$ of some glasses with different anions are presented in Fig. 7. It is remarkable that the narrow distribution of Eu^{3+} coordinated site in zinc–thallium–tellurite glass. All of the ratios for the oxide glasses are closer to the behavior predicted by the BR model than that of the fluoride glass. This difference originates probably from the difference in the electronegativities of oxygen and fluorine anions. The electronegativity (in Pauling scale) of the oxygen and fluorine are 3.44 and 3.98. Therefore, the degree of covalency in the Eu–O bond should be more than that in the Eu–F bond. According to the research of Brecher and Riseberg [21], the structural model derived for oxide glasses was found to be inadequate to explain the observed behaviors of the fluoride glasses, but an alternate model was proposed, this model involves a ninefold coordination of Eu by two set of nonequidistant fluoride ions and a systematic axial distortion of this arrangement.

The scalar crystal field strength parameter *S*, which is defined in terms of rotational invariants of the crystal field, could be calculated on the basis of the crystal field parameters following equation (see Table 2):

$$S = \left[\frac{1}{3}\sum_{n}\frac{1}{2n+1}(B_{n0})^2 + 2\sum_{m>0}((\mathrm{Re}B_{nm})^2 + (\mathrm{Im}B_{nm})^2)\right]^{1/2} \quad (4)$$

Table 2
Scalar crystal field strength *S* for a zinc–thallium–tellurite glass studied as a function of the excitation wavenumber.

Excitation energy (cm^{-1})	S (cm^{-1})
17,276	193
17,271	188
17,266	180
17,261	169
17,256	159
17,251	152
17,247	147
17,242	138
17,237	133
17,232	122
17,227	120
17,222	113
17,217	111
17,212	107
17,208	103
17,203	102
17,198	98

It could be noticed that the CF strength parameters increases with increasing excitation energy, in agreement with the BR model. The *S* values are very similar to those obtained in niobium tellurite glass [26] and in zinc tellurite glass [27]. The *S* value calculated for an excitation energy corresponding to the peak of the $^7F_0$–$^5D_0$ absorption band (S=120.6 at 17,271 cm^{-1}) is much lower than for the oxide glasses but in agreement with the other tellurite glasses [26,27].

Table 2 indicates that Eu^{3+} ions occupy mainly the weak and medium CF environments in this glass.

4. Conclusion

The analysis of the FLN spectra of zinc–thallium–tellurite glass doped with Eu^{3+} indicated that the local geometry at the lanthanide sites could be described by using the classical BR model under assumption of the C_{2v} symmetry. The crystal field strengths at various Eu^{3+} sites appeared to be lower compared to other oxide glasses. Moreover, the narrow distribution of the $-B_{22}/B_{20}$ ratio was found to be intrinsic for tellurite glasses. The obtained behaviors was quite similar to that seen for other tellurite glasses but different from those seen for silicate and fluorite glasses.

References

[1] T. Hayakawa, M. Koduka, M. Nogami, J.R. Duclère, A.P. Mirgorodsky, P. Thomas, Scr. Mater. 62 (2010) 806–809.
[2] G. Vrillet, P. Thomas, V. Couderc, A. Barthélémy, J.-C. Champarnaud-Mesjard, J. Non-Cryst. Solids 345 (2004) 417–421.
[3] M. Soulis, J.-R. Duclère, T. Hayakawa, V. Couderc, M. Dutreilh-Colas, P. Thomas, Mater. Res. Bull. 45 (2010) 551.
[4] M. Udovic, P. Thomas, A. Mirgorodsky, O. Masson, T. Merie-Mejean, C. Lasbrugnas, J.C. Champarnaud-Mesjard, T. Hayakawa, Mater. Res. Bull. 44 (2009) 248–253.
[5] B. Jeansannetas, S. Bousquet, L. Canioni, S. Le Boiteux, P. Segonds, L. Sarger, J. Solid State Chem. 146 (1999) 329–335.
[6] T. Hayakawa, M. Hayakawa, M. Nogami, P. Thomas, Opt. Mater. 32 (2010) 448–455.
[7] O. Noguera, T. Merie-Mejean, A.P. Mirgorodsky, M.M. Smirnov, P. Thomas, J.C. Champarnaud-Mejean, J. Non-Cryst. Solids 330 (2003) 50–60.
[8] M.J. Weber, in: W.M. Yen, P.M. Selzer (Eds.), Laser Spectroscopy of Solids, Springer, Berlin 1986, p. 189.
[9] B.R. Judd, Phys. Rev. 127 (1962) 750–761.

[10] G.S. Ofelt, J. Chem. Phys. 37 (1962) 511–520.
[11] T. Hayakawa, M. Nogami, J. Appl. Phys. 90 (2001) 2200–2205.
[12] R. Arafin, M.R. Sahar, Solid State Sci. Technol. 16 (2008) 29–36.
[13] A. Kumar, D.K. Rai, S.B. Rai, Spectrochim. Acta Part 58 (2002) 2115–2125.
[14] C. Goeller-Walrand, K. Binnemans, Spectral intensities of *f–f* transitions, Handbook on the Physics and Chemistry of Rare Earths, vol. 25, Chapter 167.
[15] P. Babu, C.K. Jayasankar, Physics B 279 (2000) 262–281.
[16] E.W.J.L. Oomen, A.M.A. van Dongen, J. Non-Cryst. Solids 111 (1989) 205–212.
[17] J.A. Capobianco, P.P. Proulx, M. Bettinelli, F. Negrisolo, Phys. Rev. B 42 (10) (1990) 5936–5944.
[18] M.T. Harrison, R.G. Denning, S.T. Davey, J. Non-Cryst. Solids 184 (1995) 286–291.
[19] M.T. Harrison, R.G. Denning, J. Lumin. 69 (1996) 265–285.
[20] C. Brecher, L.A. Riseberg, Phys. Rev. B 13 (1976) 81–93.
[21] C. Brecher, L.A. Riseberg, Phys. Rev. B 21 (1980) 2607–2618.
[22] A. Lempicki, H. Samelson, C. Brecher, J. Mol. Spectrosc. 27 (1968) 375–401.
[23] R. Rolli, G. Samoggia, G. Ingletto, M. Bettinelli, A. Speghini, Mater. Res. Bull. 35 (2000) 1227–1234.
[24] T.F. Belliveau, D.J. Simkin, J. Non-Cryst. Solids 110 (1989) 127–141.
[25] M. Bettinelli, A. Speghini, M. Ferrari, M. Montagna, J. Non-Cryst. Solids 201 (1996) 211–221.
[26] M. Zambelli, M. Abril, V. Lavin, A. Speghini, M. Bettinelli, J. Non-Cryst. Solids 345&346 (2004) 386–390.
[27] R. Rolli, K. Gatterer, M. Wachtler, M. Bettinelli, A. Speghini, D. Ajio, Spectrochim. Acta, A 57 (2001) 2009–2017.